

Interplay between critical and off-critical zeros of two-dimensional Epstein zeta functions

Laurent Bétermin

Institut Camille Jordan, Université Claude Bernard Lyon 1, 69622 Villeurbanne, France

Ladislav Šamaj and Igor Travěnek

Institute of Physics, Slovak Academy of Sciences, Dúbravská cesta 9, 84511 Bratislava, Slovakia

ARTICLE HISTORY

Compiled November 17, 2022

ABSTRACT

The two-dimensional Epstein zeta function associated to a rectangular lattice with spacings $a_x = 1$ and $a_y = \Delta \in \mathbb{R}_+^*$, defined by $\zeta^{(2)}(s, \Delta) = \frac{1}{2} \sum'_{j,k} (j^2 + \Delta^2 k^2)^{-s}$ ($\Re(s) > 1$), where the sum goes over all integers except of the origin $(j, k) = (0, 0)$, is studied. It can be analytically continued to the whole complex s -plane except for the point $s = 1$. The nontrivial zeros $\{\rho = \rho_x + i\rho_y\}$ of the Epstein zeta function, defined by $\zeta^{(2)}(\rho, \Delta) = 0$, split into “critical” zeros (on the critical line $\rho_x = \frac{1}{2}$) and “off-critical” zeros ($\rho_x \neq \frac{1}{2}$). This work presents rigorous asymptotic and analytic results as well as numerical investigations. According to the present numerical calculation, the critical zeros form open or closed curves $\rho_y(\Delta)$ in the plane (Δ, ρ_y) . Nearest critical zeros merge at special points (Δ^*, ρ_y^*) , referred to as left/right edge zeros, which are defined by a divergent tangent $d\rho_y/d\Delta$. Each of these critical edge zeros gives rise to a continuous curve of off-critical zeros which can thus be generated systematically. As a rule, each curve of off-critical zeros joins a pair of left and right edge zeros. It is shown that in the regions of small/large values of the anisotropy parameter Δ the Epstein zeta function can be approximated adequately by a function which reveals an equidistant distribution of critical zeros along the imaginary axis in the limits $\Delta \rightarrow 0$ and $\Delta \rightarrow \infty$. It is also numerically found that for each $\Delta \in (0, \Delta_c^*] \cup [1/\Delta_c^*, \infty)$ with $\Delta_c^* \approx 0.141733$ there exists a pair of *real* off-critical zeros, their ρ_x components going to the borders 0 and 1 of the critical region in the limits $\Delta \rightarrow 0, \infty$.

KEYWORDS

Epstein zeta function on the rectangular lattice, analytic continuation, zeros off the critical line, Jacobi theta functions

AMS CLASSIFICATION

11E45, 11M41, 11R42

1. Introduction

1.1. The zeta functions and their zeros.

We consider the two-dimensional (2D) Epstein zeta function [13, 14] associated to the rectangular lattice $a_x\mathbb{Z} \oplus a_y\mathbb{Z}$ with spacings $(a_x, a_y) = (1, \Delta)$, $\Delta \in \mathbb{R}_+^*$, defined by

$$\zeta^{(2)}(s, \Delta) := \frac{1}{2} \sum'_{(j,k) \in \mathbb{Z}^2} \frac{1}{(j^2 + \Delta^2 k^2)^s} \quad \Re(s) > 1, \quad (1.1)$$

where \sum' means that the term $(j, k) = (0, 0)$ is excluded from the summation. This represents a natural 2D extension of the one-dimensional (1D) Riemann zeta function [22] defined by

$$\zeta(s) = \frac{1}{2} \sum'_{j \in \mathbb{Z}} \frac{1}{|j|^s} = \sum_{j \in \mathbb{N}} \frac{1}{j^s}. \quad (1.2)$$

The sum (1.1) naturally arises in Physics as the energy per point of a system of identical particles located on the lattice sites of $\mathbb{Z} \oplus \Delta\mathbb{Z}$ and interacting pairwise through the Riesz potential $r \mapsto 1/r^{2s}$ [9]. Notice that the prefactor $\frac{1}{2}$ is present because each interaction energy is shared by a pair of particles.

The function $\zeta^{(2)}(s, \Delta)$ possesses the obvious symmetry

$$\zeta^{(2)}(s, \Delta) = \frac{1}{\Delta^{2s}} \zeta^{(2)}(s, 1/\Delta) \quad (1.3)$$

which means that the values of Δ can be constrained to either of the intervals $(0, 1]$ or $[1, \infty)$. Similarly as the Riemann zeta function, the Epstein zeta function can be analytically continued to the whole complex s -plane [11, 12, 13, 14]. The region $0 < \Re(s) < 1$ is referred to as the critical strip, the critical line is defined by $\Re(s) = \frac{1}{2}$.

For $\Delta^2 \in \{1, 2, 3, 4, 7\}$, the 2D lattice sum (1.1) can be expressed as a product of simpler 1D sums, namely Dirichlet L -series, whereas for other special integer values of Δ it is expressible as a *sum* of products of Dirichlet L -functions [8]. For instance, in the isotropic square lattice case $\Delta^2 = 1$, it holds

$$\zeta^{(2)}(s, 1) = 2\zeta(s)\beta(s), \quad \text{where} \quad \beta(s) := \sum_{j=0}^{\infty} \frac{(-1)^j}{(2j+1)^s} = \frac{1}{2^{2s}} \left[\zeta\left(s, \frac{1}{4}\right) - \zeta\left(s, \frac{3}{4}\right) \right] \quad (1.4)$$

is the Dirichlet beta function and $\zeta(s, a) := \sum_{j=0}^{\infty} (j+a)^{-s}$ denotes the Hurwitz zeta function.

The zeros $\{\rho = \rho_x + i\rho_y\}$ of the Epstein zeta function $s \mapsto \zeta^{(2)}(s, \Delta)$ associated to the parameter Δ are defined by the equality $\zeta^{(2)}(\rho, \Delta) = 0$. Besides the trivial zeros at $\rho \in \mathbb{Z}_-$ there exist two kinds of nontrivial zeros:

- the “critical” zeros which lie on the critical line $\rho_x = \frac{1}{2}$;
- the “off-critical” zeros which have $\rho_x \neq \frac{1}{2}$.

The Riemann hypothesis states that all nontrivial zeros of the 1D Riemann zeta function ζ are constrained to the corresponding critical line $\rho_x = \frac{1}{2}$ [22]. Provided that the Riemann hypothesis

holds, all nontrivial zeros of the Dirichlet beta function (1.4) are constrained to the critical line $\rho_x = \frac{1}{2}$ as well [18]. Consequently, all nontrivial zeros of the Epstein zeta function $\zeta^{(2)}(s, 1)$ associated to the square lattice, given by (1.4), lie on the critical line. Similar phenomenon is expected also for $\Delta^2 \in \{2, 3, 4, 7\}$ when the Epstein zeta function factorizes itself into the product of Dirichlet L -functions; for analytic and numerical studies of the statistics of gaps between critical zeros, see [2, 6, 7, 17]. This is no longer true for anisotropic (i.e. non-square) rectangular lattices (1.1) with other integer values of Δ^2 . The first off-critical zero of $\zeta^{(2)}(s, \Delta)$ was detected for $\Delta^2 = 5$ [21], since then many other off-critical zeros were identified [3, 10, 19, 24].

1.2. Main results and related works

In this paper, we perform a numerical investigation of the critical zeros of $s \mapsto \zeta^{(2)}(s, \Delta)$ for $\Delta \in (0, 1]$ in a compact set and explain how the off-critical zeros of this Epstein zeta function emerge from certain critical “edge” zeros. Most of our numerical findings are based on rigorous asymptotic and analytic results. Furthermore, we systematically check the degree of accuracy between our approximations and the direct numerical computations from more complicated equations. More precisely, our observation and results are the following:

- (1) For $\zeta^{(2)}(s, \Delta)$ one obtains numerically in the plane (Δ, ρ_y) continuous curves of critical zeros $\rho_y(\Delta)$ (remember that $\rho_x = 1/2$) and identifies critical edge zeros on them that correspond to the points of the curve with vertical tangents. These curves and critical edge zeros are depicted in Figure 1 and their construction is explained in Section 3.
- (2) The critical edge zeros are the starting points to generate systematically (here numerically) continuous curves of off-critical zeros. These continuous curves, connecting a pair of left and right edge zeros, are depicted in Figure 2 and their construction is explained in Section 4.
- (3) The analysis of the limits $\Delta \rightarrow 0$ and $\Delta \rightarrow \infty$ reveals an equidistant distribution of critical zeros along the imaginary axis, with spacing between the nearest zeros going to zero as $\mathcal{O}(1/|\log \Delta|)$. This analysis is done in Section 3.3.
- (4) A pair of real off-critical zeros is numerically found for each $\Delta \in (0, \Delta_c^*] \cup [1/\Delta_c^*, \infty)$ with $\Delta_c^* \approx 0.141733$. This is explained in Section 4.2. Furthermore, our asymptotic study for small values of Δ combined with a result by Montgomery [20] on theta functions (see also [15]) yields the following conjecture that we have also numerically checked.

Conjecture 1.1. *The unique solution of $\zeta^{(2)}(1/2, \Delta) = 0$ for $\Delta \in (0, 1)$ is $\Delta = \Delta_c^* = \frac{e^\gamma}{4\pi}$ where γ is the Euler-Mascheroni constant.*

Our work is motivated by another recent paper on d -dimensional Epstein zeta function where surprising similarities appear. Indeed, the Epstein zeta function can be defined for any lattice structure and the two last authors have recently studied in [25] the properties of the Epstein zeta function on an isotropic hypercubic lattice

$$\zeta^{(d)}(s) = \frac{1}{2} \sum'_{(n_1, n_2, \dots, n_d) \in \mathbb{Z}^d} \frac{1}{(n_1^2 + n_2^2 + \dots + n_d^2)^{s/2}} \quad \Re(s) > d, \quad (1.5)$$

where $d = 1, 2, \dots$ is the spatial dimension and the Riesz interaction energy between two particles at distance r was chosen as $1/r^s$ to reproduce in $d = 1$ the Riemann zeta function, $\zeta^{(1)}(s) = \zeta(s)$.

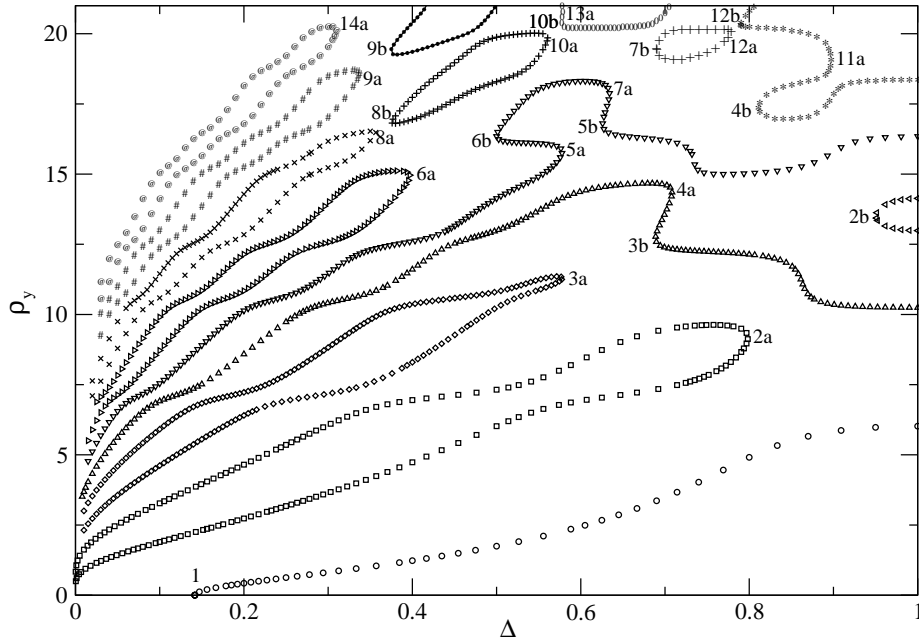


Figure 1. Numerical results for the critical zeros in the region of $0 < \Delta \leq 1$ and $0 \leq \rho_y \leq 21$. Zeros lying on the same (closed or open) curve are denoted by a common open symbol (circle, square, triangle,...). The right and left edge points are denoted as 2a, 3a, 4a,... and 1, 2b, 3b, 4b,..., respectively.

An analytic continuation of the Epstein zeta function $\zeta^{(d)}(s)$ to the whole complex s -plane was constructed; the corresponding formula is applicable for the spatial dimension d being a continuous variable ranging from 0 to ∞ . Numerical calculations of critical zeros (with $\rho_x = \frac{d}{2}$) indicate that they form closed or semi-open curves in the plane $(\rho_x = \frac{d}{2}, \rho_y)$. Each curve involves a number of left/right “edge” points at which a couple of nearest critical zeros merge. The critical edge zeros give rise to two tails of off-critical zeros, coupled via a symmetry, with continuously varying dimension d and the ρ_x -component along each tail. This fact permits one to avoid a “blind” search for off-critical zeros, the off-critical zeros are generated systematically starting from the critical edge zeros. Another benefit of the method is an exact treatment of the limits $d \rightarrow 0$ and $d \rightarrow \infty$. An exact formula for $\lim_{d \rightarrow 0} \zeta^{(d)}(s)/d$ was derived. In the limit $d \rightarrow \infty$, an equidistant distribution of critical zeros along the imaginary axis was obtained, with spacing between the nearest zeros going to zero as $2\pi/\log(d)$. As a by-product of the formalism, a conjugate pair of *real* off-critical zeros was found for each dimension $d > 9.24555\dots$

The problem of determining zeros for the d -dimensional isotropic Epstein zeta function (1.5) seems at first sight to be unrelated to that for the 2D Epstein zeta function (1.1). In analogy with [25], each of the curves of critical zeros in the (Δ, ρ_y) plane pictured in Figure 1 contains a number of left/right edge zeros. The mechanism of generation of off-critical zeros from these edge points, depicted in Figure 2 and explained in Section 4.1, is the same as in the previous case of the d -dimensional isotropic Epstein zeta function.

However, there are small differences in the form of curves of off-critical zeros. In the present 2D case, there is only one curve going out of the classical edge zero, at each point of the curve there are two conjugate off-critical zeros with ρ_x and $1 - \rho_x$ coordinates and each curve of off-critical zeros connects just one left and one right edge points. In the previous d -dimensional case, there are two tails of off-critical zeros starting at each edge point, coupled via a symmetry, and a tail

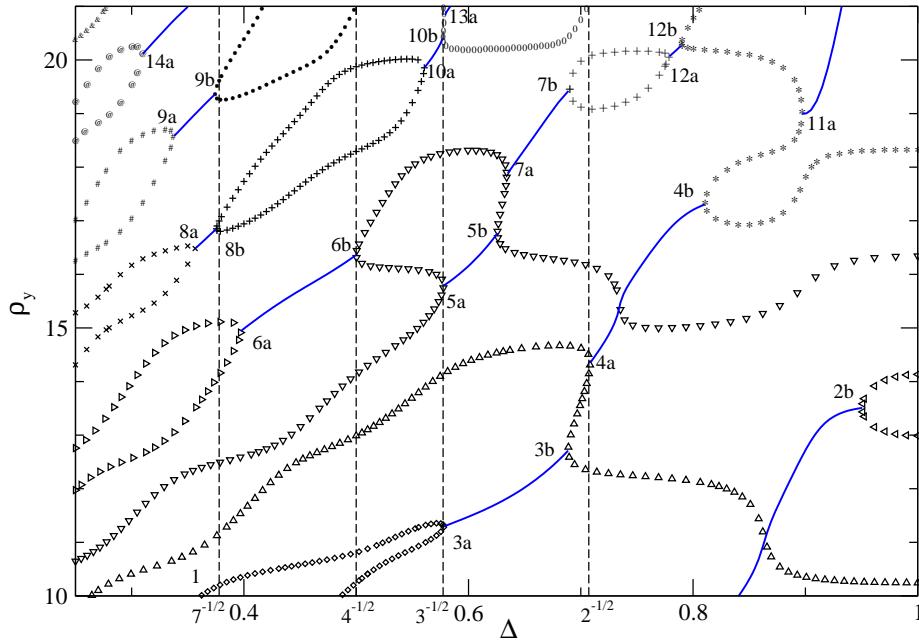


Figure 2. A fragment of Figure 1. Numerical results for solid curves of off-critical zeros interconnecting the critical right (notation “a”) and left (“b”) edge zeros. The evolution of the component ρ_x along the solid curves of off-critical zeros is not indicated. The vertical dashed lines correspond to the values of $\Delta^2 = 1, 2, 3, 4, 7$ with no off-critical zeros.

either interconnects two edge zeros or starts from one edge zero and ends at some unspecial point in $d = 0$ or $d \rightarrow \infty$ dimensions.

Another analogy with the previous paper [25] is an equidistant distribution of critical zeros along the imaginary axis in special regions of model’s parameters. In the case of the d -dimensional isotropic Epstein function (1.5), the critical zeros are distributed equidistantly in the limit $d \rightarrow \infty$ with the spacing $2\pi/\log(d)$ between the nearest-neighbor zeros. In the present case of the 2D anisotropic Epstein function (1.1), the critical zeros are distributed equidistantly in the limits $\Delta \rightarrow 0$ and $\Delta \rightarrow \infty$, with the spacing of order $\pi/|\log(\Delta)|$ between the nearest-neighbor zeros (see Section 3.3).

The next similarity with [25] consists in the appearance of a couple of real off-critical zeros with the component $\rho_y = 0$, discussed in Section 4.2.

We would like to emphasize that the presented mechanism of generation of continuous curves of off-critical zeros from the edge critical ones might be not the only possible one. Our crucial assumption was that the deviation of ρ_x from its critical value $\frac{1}{2}$ changes continuously when the off-critical zero goes out the edge zero. A discontinuous change of ρ_x was excluded from our analysis.

Plan of the paper. Section 2 concerns technicalities, like recalling the analytic continuation of the 2D Epstein zeta function $\zeta^{(2)}(s, \Delta)$ to the complex s -plane (Section 2.1) and basic equations for determining critical and off-critical zeros (Section 2.2). Section 3 deals with critical zeros of $\zeta^{(2)}(s, \Delta)$. Based on numerical calculation of open and closed curves of critical zeros in the (Δ, ρ_y) plane, the critical edge zeros are introduced in Section 3.1, together with an explicit form of two coupled integral equations determining their position in the (Δ, ρ_y) plane. The singular expansion of $\rho(y)$ around the edge points is discussed in Section 3.2. An accurate approximation of $\zeta^{(2)}(s, \Delta)$ for small (and large) values of Δ , indicating an equidistant distribution of critical

zeros along the imaginary axis, is presented in Section 3.3. Section 4 is about off-critical zeros of $\zeta^{(2)}(s, \Delta)$. The most important result of this work, the generation mechanism of curves of off-critical zeros starting from critical edge zeros, is explained in Section 4.1. Pairs of real off-critical zero are found in Section 4.2.

2. Technicalities

2.1. Regularization of $\zeta^{(2)}(s, \Delta)$

This part is devoted to a short review of the analytic continuation of the Epstein zeta function (1.1), defined when the real part $\Re(s) > 1$, to the whole complex s -plane. We have the following theorem.

Theorem 2.1 (Analytic continuation of the Epstein zeta function [5, 13]). *Let $\Delta > 0$ and $s \in \mathbb{C}$. Let us define*

$$Z(s, \Delta) := \left(\frac{\Delta}{\pi}\right)^s \Gamma(s) \zeta^{(2)}(s, \Delta). \quad (2.1)$$

We have

$$Z(s, \Delta) = -\frac{1}{2} \left(\frac{1}{1-s} + \frac{1}{s} \right) + \frac{1}{2} \int_0^1 (t^{s-1} + t^{-s}) \left[\theta_3(e^{-\pi t \Delta}) \theta_3\left(e^{-\pi t/\Delta}\right) - \frac{1}{t} \right] dt, \quad (2.2)$$

where the Jacobi elliptic theta function (with zero argument, see [16]) is given by

$$\theta_3(q) = \sum_{j \in \mathbb{Z}} q^{j^2}. \quad (2.3)$$

In particular, (2.2) represents an analytic continuation of $\zeta^{(2)}(s, \Delta)$ to the whole complex plane, except for the simple pole at $s = 1$. $Z(s, \Delta)$ fulfills the following duality relation

$$Z(s, \Delta) = Z(1-s, \Delta). \quad (2.4)$$

Remark 2.2. Note that the symmetry

$$Z(s, \Delta) = Z(s, 1/\Delta) \quad (2.5)$$

is automatically ensured by formula (2.2).

2.2. Integral equations determining zeros

We start by defining what is a zero of $s \mapsto \zeta^{(2)}(s, \Delta)$ associated to the parameter Δ .

Definition 2.1. We say that $\rho \in \mathbb{C}$ is:

- a critical zero (of $s \mapsto \zeta^{(2)}(s, \Delta)$) associated to the parameter Δ if $\rho = \frac{1}{2} + i\rho_y$, $\rho_y \in \mathbb{R}$ and $\zeta^{(2)}(\rho, \Delta) = 0$;

- an off-critical zero (of $s \mapsto \zeta^{(2)}(s, \Delta)$) associated to the parameter Δ if $\rho = \rho_x + i\rho_y$, $(\rho_x, \rho_y) \in \mathbb{R} \times \mathbb{R}$, $\rho_x \neq \frac{1}{2}$ and $\zeta^{(2)}(\rho, \Delta) = 0$.

The nontrivial zeros of $\zeta^{(2)}(s, \Delta)$ are related to the nullity condition of the right-hand side of (2.2). In the case of critical zeros $\rho = \frac{1}{2} + i\rho_y$, the right-hand side of (2.2) is real and we obtain the following result.

Theorem 2.3 (Equation for critical zeros). *Let $\rho = \frac{1}{2} + i\rho_y$ be a critical zero associated to the parameter Δ , then ρ_y satisfies the following equation:*

$$-\frac{2}{1+4\rho_y^2} + \int_0^1 \cos(\rho_y \log t) \left[\theta_3(e^{-\pi t \Delta}) \theta_3\left(e^{-\pi t/\Delta}\right) - \frac{1}{t} \right] \frac{dt}{\sqrt{t}} = 0. \quad (2.6)$$

Remark 2.4 (Symmetries of the equation and consequences). *The symmetry of (2.6) with respect to the transformation $\Delta \rightarrow 1/\Delta$ tells us that the set of critical zeros is the same for the couple of values Δ and $1/\Delta$. The symmetry $\rho_y \rightarrow -\rho_y$ means that to each critical zero $(\frac{1}{2}, \rho_y)$ there exists a complex conjugate critical zero $(\frac{1}{2}, -\rho_y)$.*

In the case of off-critical zeros with $\rho_x \neq \frac{1}{2}$, it is useful to introduce the deviation of ρ_x from its critical value

$$\delta\rho_x := \rho_x - \frac{1}{2}. \quad (2.7)$$

The right-hand side of (2.2) becomes complex in this case and the off-critical zeros are determined by a pair of coupled integral equations (corresponding to the real and imaginary parts).

Theorem 2.5 (Equation for the off-critical zeros). *Let $\rho = \frac{1}{2} + \delta\rho_x + i\rho_y$, $\delta\rho_x \neq 0$, be an off-critical zero associated to the parameter Δ , then ρ satisfies the following equations:*

$$-\left[\frac{1+2\delta\rho_x}{(1+2\delta\rho_x)^2+4\rho_y^2} + \frac{1-2\delta\rho_x}{(1-2\delta\rho_x)^2+4\rho_y^2} \right] + \int_0^1 \cos(\rho_y \log t) \cosh(\delta\rho_x \log t) \left[\theta_3(e^{-\pi t \Delta}) \theta_3\left(e^{-\pi t/\Delta}\right) - \frac{1}{t} \right] \frac{dt}{\sqrt{t}} = 0, \quad (2.8)$$

$$2\rho_y \left[\frac{1}{(1+2\delta\rho_x)^2+4\rho_y^2} - \frac{1}{(1-2\delta\rho_x)^2+4\rho_y^2} \right] + \int_0^1 \sin(\rho_y \log t) \sinh(\delta\rho_x \log t) \left[\theta_3(e^{-\pi t \Delta}) \theta_3\left(e^{-\pi t/\Delta}\right) - \frac{1}{t} \right] \frac{dt}{\sqrt{t}} = 0. \quad (2.9)$$

Furthermore, these equations are invariant with respect to the transformations $\Delta \rightarrow 1/\Delta$, $\rho_y \rightarrow -\rho_y$ and $\delta\rho_x \rightarrow -\delta\rho_x$. In particular, to each off-critical zero $(\frac{1}{2} + \delta\rho_x, \rho_y)$ there exist the related off-critical zeros $(\frac{1}{2} + \delta\rho_x, -\rho_y)$, $(\frac{1}{2} - \delta\rho_x, \rho_y)$ and $(\frac{1}{2} - \delta\rho_x, -\rho_y)$.

3. Zeros on the critical line

3.1. Critical edge zeros

Let us first comment on Figure 1. The critical zeros of the Epstein zeta function $\zeta^{(2)}(s, \Delta)$, calculated numerically by using Eq. (2.6), are represented by open symbols in Figure 1. The set of zeros lying on the same (closed or open) curve are denoted by a common open symbol (circle, square, triangle, ...). There is an infinite sequence of loop circuits in the left-down corner of the figure with the common point at the origin $(0, 0)$ which are not drawn. With regard to the symmetry $\Delta \rightarrow 1/\Delta$, each critical zero in the considered interval $\Delta \in (0, 1)$ has a counterpart in the complementary interval $(1, \infty)$. To maintain high accuracy of the results (8-20 decimal digits), only critical zeros with the component ρ_y smaller than 21 are presented. The numerical evaluation of one critical zero by using *Mathematica* takes around 5 seconds of CPU time on a conventional PC.

Each curve of critical zeros in Figure 1 is defined by the function $\rho_y(\Delta)$. Varying the parameter Δ in the positive or negative direction, the distance between a couple of nearest zeros can go to zero and the zeros merge at points referred to as the critical “edge” zeros. They originate at specific values of $\Delta = \Delta^*$ and have imaginary part $\rho_y^* = \rho_y(\Delta^*)$. More precisely, the edge zeros are defined by a divergent tangent as follows.

Definition 3.1 (Critical edge zeros). *We call (critical) edge zero any critical zero $\rho = \frac{1}{2} + i\rho_y$ such that there exists $\Delta^* > 0$ satisfying*

$$\left. \frac{d}{d\Delta} \rho_y(\Delta) \right|_{\Delta=\Delta^*} = \pm\infty. \quad (3.1)$$

Furthermore, assuming that the curve of critical zeros is defined by the inverse function $\Delta(\rho_y)$, the condition for the edge zeros (3.1) is equivalent to

$$\left. \frac{d}{d\rho_y} \Delta(\rho_y) \right|_{\rho_y=\rho_y^*} = 0 \quad (3.2)$$

and $\Delta^* = \Delta(\rho_y^*)$.

The edge zeros split into two groups: the left/right edge zeros are situated on the left/right with respect to the curve $\rho_y(\Delta)$. More precisely:

Definition 3.2 (Left/right critical edge zeros). *Let $\rho^* = \frac{1}{2} + i\rho_y^*$ be a (critical) edge zero associated to the parameter Δ^* and the curve of critical zeros is defined by the inverse function $\Delta(\rho_y)$. We say that ρ is a right (resp. left) edge zero if*

$$\left. \frac{d^2}{d\rho_y^2} \Delta(\rho_y) \right|_{\rho_y=\rho_y^*} < 0 \quad \left(\text{resp. } \left. \frac{d^2}{d\rho_y^2} \Delta(\rho_y) \right|_{\rho_y=\rho_y^*} > 0 \right).$$

The right and left edge zeros are denoted in Figure 1 as 2a, 3a, 4a, ... and 1, 2b, 3b, 4b, ..., respectively; the close connection between the right and left edge zeros 2a-2b, 3a-3b, etc. will become clear later (see Section 4.1). Notice that the critical zero numbered 1 with coordinates $(\Delta^*, \rho_y^*) = (\Delta_c^* \approx 0.141733, 0)$ is a left edge zero because the corresponding curve continues

reflection-symmetrically across the Δ -axis into the lower quadrant.

We can easily deduce closed-form equations for specifying edge zeros.

Theorem 3.1 (Equation satisfied by a critical edge zero). *If $\rho^* = \frac{1}{2} + i\rho_y^*$ is an edge zero associated to the parameter Δ^* , then*

$$f(\rho_y^*, \Delta^*) = 0, \quad (3.3)$$

where the function f is given by

$$f(\rho_y, \Delta) := \frac{16\rho_y}{(1 + 4\rho_y^2)^2} - \int_0^1 \log t \sin(\rho_y \log t) \left[\theta_3(e^{-\pi t \Delta}) \theta_3(e^{-\pi t / \Delta}) - \frac{1}{t} \right] \frac{dt}{\sqrt{t}}. \quad (3.4)$$

Proof. We first recall that an edge zero has to satisfy the general equation (2.6) for critical zeros, i.e.,

$$-\frac{2}{1 + 4\rho_y^{*2}} + \int_0^1 \cos(\rho_y^* \log t) \left[\theta_3(e^{-\pi t \Delta^*}) \theta_3(e^{-\pi t / \Delta^*}) - \frac{1}{t} \right] \frac{dt}{\sqrt{t}} = 0. \quad (3.5)$$

Taking into account the edge-zero condition (3.2), the derivative of (2.6) with respect to ρ_y leads to the result. \square

It has to be noticed that the coupled equations (3.3) and (3.5) have an infinite number of real solutions for Δ^* and ρ_y^* . The characteristics of edge critical zeros from Figure 1, constrained to the intervals $0 < \Delta \leq 1$ and $0 \leq \rho_y \leq 21$, are summarized in Table 1.

3.2. Singular expansion around critical edge zeros

The map $\Delta \mapsto \rho_y(\Delta)$ exhibits locally an analytic expansion in Δ , except for the edge zeros where it shows a singular expansion in Δ . The singular expansion around edge zeros can be documented by performing the Taylor series expansion of the inverse function $\Delta(\rho_y)$ on the corresponding curve of critical zeros. We obtain the following result.

Lemma 3.2 (First order asymptotics around a critical edge zero). *Let $\rho^* = \frac{1}{2} + i\rho_y^*$ be an edge zero associated to the parameter Δ^* . Then, as $\rho_y \rightarrow \rho_y^*$ where $\rho = \frac{1}{2} + i\rho_y$ is a critical zero associated to the parameter Δ , we have*

$$\rho_y - \rho_y^* = \mathcal{O}\left(\sqrt{|\Delta - \Delta^*|}\right).$$

Proof. The result directly follows from the order two Taylor expansion of the inverse function $\Delta(\rho_y)$ given by

$$\Delta(\rho_y) = \Delta(\rho_y^*) + \frac{1}{2!} \frac{d^2}{d\rho_y^2} \Delta(\rho_y) \Big|_{\rho_y = \rho_y^*} (\rho_y - \rho_y^*)^2 + o\left((\rho_y - \rho_y^*)^2\right), \quad (3.6)$$

where the condition (3.2) was taken into account. \square

Table 1. The coordinates of edge critical zeros appearing in the region of $0 < \Delta \leq 1$ and $0 \leq \rho_y \leq 21$ in Figure 1.

edge point	Δ^*	ρ_y^*
1	0.141733239663887	0
2a	0.798382429865856	9.17479405815734
2b	0.950672823506692	13.5092488680816
3a	0.578095740200051	11.2961629757333
3b	0.688797339793161	12.7134082666419
4a	0.708261915413478	14.3461052173020
4b	0.810471985748564	17.3035168808027
5a	0.577833206956181	15.7904269230734
5b	0.625830051933379	16.7721421891791
6a	0.397042034784957	14.9386821841068
6b	0.499955572107973	16.3629327845743
7a	0.634086781531453	17.8588321271621
7b	0.690295752437308	19.4462462865857
8a	0.356573014664413	16.4816098051657
8b	0.375454386384881	16.8495675287149
9a	0.337272867689201	18.5674591768417
9b	0.374296061779980	19.3629136770424
10a	0.560652822542094	19.8540419510498
10b	0.577320038404815	20.4237238736290
11a	0.896821462590355	19.0008766867965
12a	0.778481639573212	20.0611304186419
12b	0.789270563104711	20.2667094854061
13a	0.578437965650995	20.8178435639014
14a	0.309679721075915	20.1102459521285

We now perform a general analysis for critical zeros, deriving an asymptotic expansion of Equation (2.6) around a critical zero $\rho = \frac{1}{2} + i\rho_y$ associated to the parameter Δ .

Lemma 3.3 (Asymptotic expansion around a general critical zero). *Let $\rho = \frac{1}{2} + i\rho_y$ and $\tilde{\rho} = \frac{1}{2} + i(\rho_y + \delta\rho_y)$ be two critical zeros respectively associated to the parameters Δ and $\Delta + \delta\Delta$. Then we have, as $\delta\Delta \rightarrow 0$ (and therefore $\delta\rho_y \rightarrow 0$),*

$$a\delta\Delta + f\delta\rho_y + c(\delta\rho_y)^2 - b(\delta\Delta)(\delta\rho_y) - d(\delta\rho_y)^3 + \mathcal{O}[(\delta\Delta)^2] + \mathcal{O}[\delta\Delta(\delta\rho_y)^2] = 0, \quad (3.7)$$

where the function $f = f(\rho_y, \Delta)$ is defined by (3.4) and the other prefactor functions a, b, c and d , depending on (ρ_y, Δ) , are given by

$$a = \pi \int_0^1 \sqrt{t} \cos(\rho_y \log t) \left[\theta_3(e^{-\pi t \Delta}) \frac{1}{\Delta^2} \vartheta(e^{-\pi t/\Delta}) - \theta_3(e^{-\pi t/\Delta}) \vartheta(e^{-\pi t \Delta}) \right] dt, \quad (3.8)$$

$$b = \pi \int_0^1 \sqrt{t} \sin(\rho_y \log t) (\log t) \left[\theta_3(e^{-\pi t \Delta}) \frac{1}{\Delta^2} \vartheta(e^{-\pi t/\Delta}) - \theta_3(e^{-\pi t/\Delta}) \vartheta(e^{-\pi t \Delta}) \right] dt, \quad (3.9)$$

$$c = \frac{8(1 - 12\rho_y^2)}{(1 + 4\rho_y^2)^3} - \frac{1}{2} \int_0^1 \cos(\rho_y \log t) (\log t)^2 \left[\theta_3(e^{-\pi t \Delta}) \theta_3(e^{-\pi t/\Delta}) - \frac{1}{t} \right] \frac{dt}{\sqrt{t}}, \quad (3.10)$$

$$d = \frac{128\rho_y(1 - 4\rho_y^2)}{(1 + 4\rho_y^2)^4} - \frac{1}{6} \int_0^1 \sin(\rho_y \log t) (\log t)^3 \left[\theta_3(e^{-\pi t \Delta}) \theta_3(e^{-\pi t/\Delta}) - \frac{1}{t} \right] \frac{dt}{\sqrt{t}} \quad (3.11)$$

with θ_3 is defined by (2.3) and

$$\vartheta(q) := q \frac{d}{dq} \theta_3(q) = \sum_{j \in \mathbb{Z}} j^2 q^{j^2}. \quad (3.12)$$

Proof. One substitutes

$$\Delta \rightarrow \Delta + \delta\Delta, \quad \text{and} \quad \rho_y \rightarrow \rho_y + \delta\rho_y \quad (3.13)$$

into equation (2.6) and expands in Taylor series in powers of small deviations $\delta\Delta$ and $\delta\rho_y$. Furthermore, the θ_3 -functions appearing in (2.6) are expanded as follows

$$\theta_3(e^{-\pi t \Delta}) \rightarrow \theta_3(e^{-\pi t \Delta}) - \pi t (\delta\Delta) \vartheta(e^{-\pi t \Delta}), \quad \theta_3(e^{-\pi t/\Delta}) \rightarrow \theta_3(e^{-\pi t/\Delta}) + \frac{\pi t \delta\Delta}{\Delta^2} \vartheta(e^{-\pi t/\Delta}). \quad (3.14)$$

It is now straightforward to obtain the desired result. \square

It is easy to derive the following asymptotics for $\delta\rho_y$ in the case of a critical zero which does not belong to the set of edge zeros.

Lemma 3.4 (Asymptotic expansion around a critical non-edge zero). *Let $\rho = \frac{1}{2} + i(\rho_y + \delta\rho_y)$ be a critical zero associated to the parameter $\Delta + \delta\Delta$ such that the critical zero $\frac{1}{2} + i\rho_y$ associated to the parameter Δ is not an edge zero. Then we have, as $\delta\Delta \rightarrow 0$ (and consequently $\delta\rho_y \rightarrow 0$),*

$$\delta\rho_y = -\frac{a}{f} \delta\Delta + \mathcal{O}(\delta\rho_y \delta\Delta).$$

Proof. Since ρ is not an edge zero, we have $f(\rho_y, \Delta) \neq 0$ and therefore the leading term of the expansion of the deviation $\delta\rho_y$ in small $\delta\Delta$ is determined by the equation $a\delta\Delta + f\delta\rho_y + \mathcal{O}(\delta\rho_y \delta\Delta) = 0$, which leads to our result. \square

We can also derive from (3.7) the following asymptotics around an edge zero.

Lemma 3.5 (Asymptotic expansion around a critical edge zero). *Let $\rho = \frac{1}{2} + i(\rho_y^* + \delta\rho_y)$ associated to the parameter Δ be a critical zero where $\rho^* = \frac{1}{2} + i\rho_y^*$, associated to the parameter Δ^* with $\Delta > \Delta^*$, is a left edge zero. Then we have, as $\Delta \rightarrow \Delta^*$ (and therefore $\rho_y \rightarrow \rho_y^*$),*

$$\rho_y(\Delta) = \rho_y(\Delta^*) \pm \sqrt{-\frac{a}{c} \sqrt{\Delta - \Delta^*} + \frac{1}{2c} \left(b - \frac{ad}{c} \right) (\Delta - \Delta^*)} + \mathcal{O} \left[(\Delta - \Delta^*)^{3/2} \right], \quad (3.15)$$

where the sign \pm determines the up/down branches of $\rho_y(\Delta)$.

Remark 3.6. In particular, the leading order term of our asymptotics is given, as $\Delta \rightarrow \Delta^*$, by

$$\rho_y(\Delta) = \rho_y(\Delta^*) \pm \sqrt{-\frac{a}{c}} \sqrt{\Delta - \Delta^*} + o\left(\sqrt{\Delta - \Delta^*}\right). \quad (3.16)$$

Here, the ratio $-a/c$ must be positive for the real component ρ_y to exist and it was checked numerically for all left edge zeros presented in Table 1 that it is so. Notice that singular expansion of type (3.16) with the critical exponent $\frac{1}{2}$ occurs in a mean-field description of classical statistical systems at the second-order phase transition [4, 23]. An analogous analysis can be done for right edge zeros.

Proof. For a critical edge zero $\rho^* = \frac{1}{2} + i\rho_y^*$, the linear term of order $\delta\rho_y$ is absent in (3.7) since $f(\rho_y^*, \Delta^*) = 0$. Terms on the left-hand side of (3.7) can be classified according to their power in the smallness parameter $\delta\Delta$ and the leading order can be easily derived. To go to the next order in $\delta\Delta$, one adds to $\delta\rho_y$ in (3.16) a higher-order term $\alpha\delta\Delta$ with the as-yet-undetermined constant α . Expanding all functions in (3.7) up to the order $(\delta\Delta)^{3/2}$ one ends up with the relation $2c\alpha - b + ad/c = 0$ which fixes α . It is now straightforward to get our final expression of the asymptotics. \square

Application and comparison with the direct computations. Let us choose one of the left edge critical zeros in Figure 1, say the edge point 3b with characteristics Δ^* and ρ_y^* listed in Table 1. After the numerical evaluation of the coefficients a, b, c and d , the expansion (3.15) takes the form

$$\delta\rho_y(\Delta) = \pm 4.87411\sqrt{\Delta - \Delta^*} + 22.493(\Delta - \Delta^*) + \mathcal{O}\left[(\Delta - \Delta^*)^{3/2}\right]. \quad (3.17)$$

The fitting of numerical data for the up branch (the + sign) implies the prefactor 4.87412 to $\sqrt{\Delta - \Delta^*}$ and the one 22.686 to $(\Delta - \Delta^*)$, while for the down branch (the - sign) the corresponding prefactors -4.87415 and 22.230 deviate a bit more from the “exact” ones in (3.17), but they are still suitable.

3.3. Approximation of Epstein zeta function for small values of Δ

In this part, for small values of the anisotropy parameter Δ , the Epstein function is approximated well by a function which reveals an equidistant distribution of critical zeros along the imaginary axis in the limit $\Delta \rightarrow 0$. We start by showing the following asymptotic result as $\Delta \rightarrow 0$.

Theorem 3.7 (Asymptotics for small values of Δ). As $\Delta \rightarrow 0$, we have

$$\zeta^{(2)}(s, \Delta) = \frac{1}{\Delta^{2s}} \frac{1}{\pi^{\frac{1}{2}-2s}} \frac{\Gamma\left(\frac{1}{2}-s\right)}{\Gamma(s)} \zeta(1-2s) + \frac{1}{\Delta} \frac{\sqrt{\pi}\Gamma\left(s-\frac{1}{2}\right)}{\Gamma(s)} \zeta(2s-1) + \mathcal{O}(\Delta). \quad (3.18)$$

Proof. The sum in (1.1) can be straightforwardly converted to

$$\frac{1}{2} \sum'_{j,k=-\infty}^{\infty} \frac{1}{(j^2 + \Delta^2 k^2)^s} = \zeta(2s) + \frac{1}{\Delta^{2s}} \zeta(2s) + 2 \sum_{j,k=1}^{\infty} \frac{1}{(j^2 + \Delta^2 k^2)^s}. \quad (3.19)$$

Writing

$$\sum_{k=1}^{\infty} \frac{1}{(j^2 + \Delta^2 k^2)^s} = \sum_{k=0}^{\infty} \frac{1}{(j^2 + \Delta^2 k^2)^s} - \frac{1}{j^{2s}} \quad (3.20)$$

the Epstein zeta function is expressed as

$$\zeta^{(2)}(s, \Delta) = \frac{1}{\Delta^{2s}} \zeta(2s) - \zeta(2s) + \sum_{j=1}^{\infty} \sum_{k=0}^{\infty} f_j(k), \quad (3.21)$$

where

$$f_j(x) = \frac{2}{(j^2 + \Delta^2 x^2)^s}. \quad (3.22)$$

In the limit $\Delta \rightarrow 0$, the difference between successive terms in the sum $\sum_{k=0}^{\infty} f_j(k)$ is also negligibly small. The sum can be thus treated as an integral according to the Euler-Maclaurin formula [1]

$$\sum_{k=0}^{\infty} f_j(k) = \int_0^{\infty} f_j(x) dx + \frac{f_j(0) + \lim_{M \rightarrow \infty} f_j(M)}{2} + \sum_{l=1}^{\lfloor \frac{p}{2} \rfloor} \frac{B_{2l}}{(2l)!} \left[\lim_{M \rightarrow \infty} f_j^{(2l-1)}(M) - f_j^{(2l-1)}(0) \right] + R_j(p), \quad (3.23)$$

where $p \geq 2$ is an integer, $[\dots]$ denotes the integer part, $\{B_{2l}\}$ are Bernoulli numbers and the absolute value of the error term $R_j(p)$ is bounded by

$$|R_j(p)| \leq \frac{2\zeta(p)}{(2\pi)^p} \int_0^{\infty} |f_j^{(p)}(x)| dx. \quad (3.24)$$

$f_j(x)$ is an even function of x and therefore its odd derivatives with respect to x vanish at $x = 0$. Since the derivatives of $f_j(x)$ vanish also at $x \rightarrow \infty$, it holds that

$$\sum_{k=0}^{\infty} f_j(k) = 2 \int_0^{\infty} \frac{dx}{(j^2 + \Delta^2 x^2)^s} + \frac{1}{j^{2s}} + R_j(p). \quad (3.25)$$

Evaluating the integral

$$\int_0^{\infty} \frac{dx}{(j^2 + \Delta^2 x^2)^s} = \frac{1}{\Delta} \frac{1}{j^{2s-1}} \frac{\sqrt{\pi} \Gamma(s - \frac{1}{2})}{2 \Gamma(s)}, \quad (3.26)$$

we end up with

$$\zeta^{(2)}(s, \Delta) = \frac{1}{\Delta^{2s}} \zeta(2s) + \frac{1}{\Delta} \frac{\sqrt{\pi} \Gamma(s - \frac{1}{2})}{\Gamma(s)} \zeta(2s - 1) + \sum_{j=1}^{\infty} R_j(p). \quad (3.27)$$

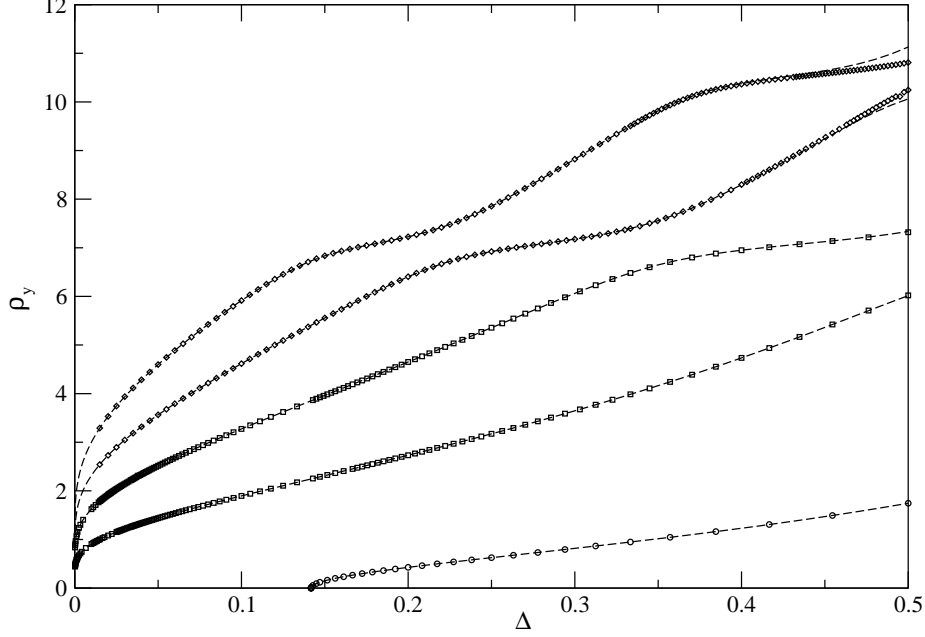


Figure 3. The comparison of the results for the first critical zeros as the functions of Δ calculated from the approximative equation (3.33) (dashed curves) with the ones obtained by using the exact equation (2.6) (the symbol notation is taken from Figure 1).

By applying the dual relation (see e.g. [5])

$$\frac{1}{\pi^s} \Gamma(s) \zeta(2s) = \frac{1}{\pi^{\frac{1}{2}-s}} \Gamma\left(\frac{1}{2} - s\right) \zeta(1 - 2s) \quad (3.28)$$

we end up with the following asymptotic expansion as $\Delta \rightarrow 0$:

$$\zeta^{(2)}(s, \Delta) = \frac{1}{\Delta^{2s}} \frac{1}{\pi^{\frac{1}{2}-2s}} \frac{\Gamma\left(\frac{1}{2} - s\right)}{\Gamma(s)} \zeta(1 - 2s) + \frac{1}{\Delta} \frac{\sqrt{\pi} \Gamma\left(s - \frac{1}{2}\right)}{\Gamma(s)} \zeta(2s - 1) + \sum_{j=1}^{\infty} R_j(p). \quad (3.29)$$

To estimate the error term, writing $s = s_x + is_y$, we insert $f_j(x)$ (3.22) into the bound (3.24) for $p = 2$ and obtain by a straightforward computation that

$$\left| \sum_{j=1}^{\infty} R_j(2) \right| \leq \sum_{j=1}^{\infty} \frac{2\zeta(2)}{(2\pi)^2} \int_0^{\infty} |f_j^{(2)}(x)| dx = \frac{8\Delta\zeta(2)\zeta(2s_x + 1)}{(2\pi)^2} \sqrt{s_x^2 + s_y^2} I(s_x, s_y), \quad (3.30)$$

where the integral

$$I(s_x, s_y) = \int_0^1 \left\{ \sqrt{[1 - (1 + 2s_x)t^2]^2 + 4s_y^2 t^4} + t^{2s_x} \sqrt{[t^2 - (1 + 2s_x)]^2 + 4s_y^2} \right\} \frac{dt}{(1 + t^2)^{2+s_x}} \quad (3.31)$$

converges if $s_x > -\frac{1}{2}$. Note that $\zeta(2s_x + 1)$ diverges for $s_x = 0$. This completes the proof. \square

Table 2. The comparison of the exact and approximate values of the first 8 zeros for $\Delta = 1/\sqrt{7}$.

zero #	ρ_y exact	ρ_y approx
1	1.133090035457	1.133090358285
2	4.475738283729	4.475726461185
3	6.845491712491	6.845712742060
4	7.931630248198	7.930996972746
5	10.19781031911	10.20336832640
6	11.16018454312	11.14537554655
7	12.48960334303	12.51829228147
8	14.13472514173	14.05004856679

Remark 3.8. The expansion (3.29) then has the meaning of a systematic Laurent series expansion in Δ provided that $\Re(s) > 0$.

Approximate equation for zeros in the small Δ regime and comparison with direct computations. Let us neglect the error term of order Δ and consider the approximate equation for zeros $\{\rho\}$ of the Epstein zeta function in the region of small Δ :

$$\left(\frac{\Delta}{\pi}\right)^{2\rho-1} = -\frac{\Gamma\left(\frac{1}{2}-\rho\right)\zeta(1-2\rho)}{\Gamma\left(\rho-\frac{1}{2}\right)\zeta(2\rho-1)}. \quad (3.32)$$

For the critical zeros $\rho = \frac{1}{2} + i\rho_y$, this equation takes the form

$$\left(\frac{\Delta}{\pi}\right)^{2i\rho_y} = -\frac{\Gamma(-i\rho_y)\zeta(-2i\rho_y)}{\Gamma(i\rho_y)\zeta(2i\rho_y)}. \quad (3.33)$$

In Figure 3, the results for the first critical zeros as the functions of the anisotropy parameter Δ calculated from this approximative equation (dashed curves) are compared with the ones obtained by using the exact equation (2.6) (the symbol notation is taken from Figure 1). It is seen that the critical zeros obtained from the approximate equation (3.33) agree with the exact ones unexpectedly far away, up to $\Delta \approx 0.5$. Roughly speaking, the approximate formula (3.33) works well until approaching an edge zero at which two critical zeros merge, the phenomenon which is out of reach of this formula. This can be seen in the upper right corner of Fig. 3 where the two “exact” curves tend to the right edge point 3a. High accuracy of the approximative values of the first eight critical zeros for the Epstein zeta function is documented for $\Delta = 1/\sqrt{7} \approx 0.378$ in Table 2. As is intuitively expected, the accuracy of the approximative results deteriorates as the value of ρ_y increases.

The following result illustrates what we observe on Figure 3 and shows that, in the limit $\Delta \rightarrow 0$, the set of critical zeros is equidistant along the imaginary axis, with the spacing $\frac{\pi}{|\log(\Delta/\pi)|}$ between the nearest neighbors.

Lemma 3.9 (Asymptotic behavior of ρ_y as $\Delta \rightarrow 0$). Let $\rho = \frac{1}{2} + i\rho_y$ be a critical zero associated to the parameter Δ . Then we have

$$\lim_{\Delta \rightarrow 0} \rho_y(\Delta) = 0.$$

Furthermore, in the limit $\Delta \rightarrow 0$, the asymptotic critical zeros are given by $\{\rho(n) := \frac{1}{2} + \rho_y(n)\}$ where

$$\rho_y(n) := \frac{\pi n}{|\log(\Delta/\pi)|}, \quad n \in \mathbb{Z}^*. \quad (3.34)$$

Proof. Let us consider the two first orders of the asymptotics in (3.29) when $s = \frac{1}{2} + i\rho_y$:

$$\zeta^{(2)}(s, \Delta) = \frac{\sqrt{\pi}\Gamma(-i\rho_y)\zeta(-2i\rho_y)}{\Delta\Gamma(\frac{1}{2} + i\rho_y)} \left[\left(\frac{\Delta}{\pi}\right)^{-2i\rho_y} + \frac{\Gamma(i\rho_y)\zeta(2i\rho_y)}{\Gamma(-i\rho_y)\zeta(-2i\rho_y)} \right]. \quad (3.35)$$

Let us assume that in the limit $\Delta \rightarrow 0$ also the component ρ_y of critical zeros goes to 0, as is seen in Figure 3. Since

$$\lim_{\rho_y \rightarrow 0} \frac{\Gamma(i\rho_y)\zeta(2i\rho_y)}{\Gamma(-i\rho_y)\zeta(-2i\rho_y)} = -1, \quad (3.36)$$

the critical zeros are given by $(\Delta/\pi)^{2i\rho_y} = 1$, in agreement with (3.34). As

$$\frac{\sqrt{\pi}\Gamma(-i\rho_y)\zeta(-2i\rho_y)}{\Delta\Gamma(\frac{1}{2} + i\rho_y)} \underset{\rho_y \rightarrow 0}{\sim} -\frac{i}{2\rho_y}, \quad (3.37)$$

the zeta function $\zeta^{(2)}(\frac{1}{2} + \rho_y, \Delta)$ diverges as $|\log \Delta|/\Delta$ on the curves of critical zeros as $\Delta \rightarrow 0$, but this has no impact on the location of its zeros. The proof is complete. \square

The distance between the nearest neighbors in the asymptotic sequence of critical zeros (3.34) is predicted to be $\pi/|\log(\Delta/\pi)|$; the dependence on the inverse of $\log(\Delta)$ indicates that one has to take extremely small values of Δ to obtain reliable results. We have performed numerical evaluation of the first few critical zeros with $\rho_y > 0$ for $\Delta = 0.0001$ by using the exact formula (2.6). The distance between the first and second zeros is 0.375, between the second and third zeros is 0.357, between the third and fourth zeros is 0.347, between the fourth and fifth zeros is 0.340, between the fifth and sixth zeros is 0.337, etc., which means that the spectrum of zeros is almost equidistant as was anticipated. Our asymptotic result (3.34) suggests that the distance should be 0.303 which is a reasonable estimate for the considered (not small enough) value of $\Delta = 0.0001$.

Remark 3.10 (The large Δ case). *With regard to the symmetry $\Delta \rightarrow 1/\Delta$ of basic equations (2.6) for critical and (2.8), (2.9) for off-critical zeros, one can accomplish an analogous analysis in the opposite limit $\Delta \rightarrow \infty$, with the result*

$$(\pi\Delta)^{2\rho-1} = -\frac{\Gamma(\rho - \frac{1}{2})\zeta(2\rho - 1)}{\Gamma(\frac{1}{2} - \rho)\zeta(1 - 2\rho)}. \quad (3.38)$$

Similarly as in the limit $\Delta \rightarrow 0$, the spectrum of critical zeros is equidistant along the imaginary axis in the limit $\Delta \rightarrow \infty$, with the spacing $\frac{\pi}{\log(\pi\Delta)}$ between the nearest neighbors.

4. Zeros off the critical line

4.1. Generation of off-critical zeros from critical edge zeros

We observe the following in Figure 1: given an edge zero associated to the parameter Δ^* , there exists $\delta_0 > 0$ such that for all $0 < \delta < \delta_0$, for a left (resp. right) edge zero, there is no critical zero associated to the parameter $\Delta^* - \delta$ (resp. $\Delta^* + \delta$). In the specific case of left edge zeros, this is caused by the fact that Eq. (3.7) with the numerically verified inequality $-a/c > 0$ has no real solution for $\delta\rho_y$ if $\delta\Delta = \Delta - \Delta^* < 0$, see also Eq. (3.16).

Therefore, the only way to have a zero of $\zeta^{(2)}(s, \Delta)$ corresponding to these values of the parameter Δ close to an edge zero is to allow the ρ_x -component to deviate from its critical value $\frac{1}{2}$. We therefore obtain the following result.

Lemma 4.1 (Asymptotic expansion of an off-critical zero around a critical zero). *Let $\rho = \frac{1}{2} + \delta\rho_x + i(\rho_y + \delta\rho_y)$ be an off-critical zero associated to the parameter $\Delta + \delta\Delta$ such that $\tilde{\rho} = \frac{1}{2} + i\rho_y$ is a critical zero associated to the parameter Δ . Then we have, as $\delta\Delta \rightarrow 0$ (and therefore $\delta\rho_y \rightarrow 0$ and $\delta\rho_x \rightarrow 0$), the following two equations:*

$$a\delta\Delta + f\delta\rho_y - c(\delta\rho_x)^2 + c(\delta\rho_y)^2 - b\delta\Delta\delta\rho_y + 3d(\delta\rho_x)^2\delta\rho_y - d(\delta\rho_y)^3 + o(\delta\rho_y^3) = 0, \quad (4.1)$$

$$\delta\rho_x \left[-f + b\delta\Delta - 2c\delta\rho_y - d(\delta\rho_x)^2 + 3d(\delta\rho_y)^2 + o(\delta\rho_y^2) + o(\delta\rho_x^2) \right] = 0, \quad (4.2)$$

where the function f is defined by (3.4) and the functions a , b , c and d by equations (3.8)–(3.11). Furthermore if $\tilde{\rho}$ is not an edge zero, then there is no such off-critical zero ρ in its neighborhood.

Proof. We simply use (3.13) in (2.8) and (2.9) and Taylor expanding in powers of small variables $\delta\Delta$, $\delta\rho_x$ and $\delta\rho_y$. Furthermore, if the critical zero $\tilde{\rho}$ is not an edge zero, it holds that $f(\rho_y, \Delta) \neq 0$. The second equation (4.2) with sufficiently small $\delta\Delta$ and $\delta\rho_y$ has the only solution $\delta\rho_x = 0$. In other words, there are no off-critical zeros in the neighborhood of the critical zero which is not an edge zero. \square

Lemma 4.2 (Asymptotic expansion of an off critical zero around a left edge zero). *Let $\rho = \frac{1}{2} + \delta\rho_x + i(\rho_y^* + \delta\rho_y)$ be an off-critical zero associated to the parameter Δ such that $\rho^* = \frac{1}{2} + i\rho_y^*$ is a left edge zero associated to the parameter Δ^* . Then, we obtain, for $\Delta < \Delta^*$, $\Delta \rightarrow \Delta^*$ (and then $\delta\rho_y \rightarrow 0$ and $\delta\rho_x \rightarrow 0$),*

$$\delta\rho_x = \pm \sqrt{-\frac{a}{c}\sqrt{\Delta^* - \Delta}} + o\left(\sqrt{\Delta^* - \Delta}\right), \quad (4.3)$$

and

$$\delta\rho_y = -\frac{1}{2c} \left(b - \frac{ad}{c} \right) (\Delta^* - \Delta) + o(\Delta^* - \Delta), \quad (4.4)$$

Remark 4.3. *The relations (4.3) and (4.4) are the asymptotic formulas for a curve of off-critical zeros starting from the considered left edge point which are valid for Δ close to Δ^* and ρ_y close to ρ_y^* .*

The \pm sign for $\delta\rho_x$ in (4.3) means that at each point along a curve of off-critical zeros $\rho_y(\Delta)$ there exist a conjugate pair of solutions $\rho_x = \frac{1}{2} + \delta\rho_x$ and $1 - \rho_x = \frac{1}{2} - \delta\rho_x$. A similar analysis can be made for right edge zeros.

Proof. Since ρ^* is an edge zero, we have $f(\rho_y^*, \Delta^*) = 0$ and it follows that (4.2) is satisfied also for $\delta\rho_x \neq 0$. Indeed, note that in the first equation (4.1) the term $c(\delta\rho_y)^2$, which was dominant in the previous analysis of critical zeros in Section 3.2, has a counterpart with the opposite sign $-c(\delta\rho_x)^2$. This latter term becomes dominant when the difference $\delta\Delta = \Delta - \Delta^*$ changes its positive sign to the negative one, implying that

$$a(\Delta - \Delta^*) - c(\delta\rho_x)^2 + c(\delta\rho_y)^2 + o(\delta\rho_y^2) + o(\delta\rho_x^2) = 0,$$

Since $\delta\rho_x \neq 0$, the second equation (4.2) implies that

$$b(\Delta - \Delta^*) - 2c\delta\rho_y - d(\delta\rho_x)^2 + o((\Delta^* - \Delta)^2) + o(\delta\rho_x^2) = 0.$$

These two equations exhibit the solutions with expansions of type (4.3) and (4.4). \square

Numerical method to generate off-critical zeros curves. The fact that each curve of off-critical zeros starts/ends at edge points simplifies very much the numerical evaluation of off-critical zeros by using *Mathematica*. As a function to deal with we take the sum of the squared left-hand side of Eqs. (2.8) and (2.9). Applying the command FindMinimum to this function, the zero is taken as sure if the function value is less than 10^{-23} . To avoid escape from a local minimum, one starts from a (say right) edge point and increases Δ by a tiny amount 0.0001, after few steps the shift can be augmented to 0.001 – 0.01. The search for a minimum takes around 60 sec of CPU time on a conventional PC. For integer values of $\Delta^2 = 5, 6, 8, \dots$, when off-critical zeros can be calculated with a high precision from exact sums of products of Dirichlet L -functions [8], our numerical results agree with these analytic predictions by at least 20 decimal digits.

Numerical observations. As is seen in Figure 2, each curve of off-critical zeros joins a pair of critical right (notation “a”) and left (“b”) edge zeros. As a rule, the ρ_y -coordinate of the right edge point is smaller than that of the corresponding left edge point. In the large majority of cases the curves of off-critical zeros go up monotonously when increasing Δ ; the only exception from the curves presented in Figure 2 is the curve starting at the right edge point 11a which first goes down in a short interval of Δ -values and then goes up to the left edge point 11b (not in the figure). The intersection of a solid curve of off-critical zeros with a curve of critical zeros (symbols) is not contradictory: the component ρ_x varies along the solid curves (not indicated in the figure) while it is constant $\frac{1}{2}$ along the critical curves. The vertical dashed lines, pictured at the values $1/\sqrt{2}$, $1/\sqrt{3}$, $1/\sqrt{4}$ and $1/\sqrt{7}$ of Δ , correspond, together with $\Delta = 1$, to the special cases when $\zeta^{(2)}(s, \Delta)$ factorizes itself into product of a zeta function, a Dirichlet L function and a prefactor function whose zeros (lying on the critical line only) can be determined analytically [8, 19]. According to the generalized Riemann hypothesis [10, 19], $\zeta^{(2)}(s, \Delta)$ exhibits only critical zeros for these values of Δ . This fact is clearly seen in Figure 2 where no solid curve of off-critical zeros intersects dashed and $\Delta = 1$ lines, although some of the edge zeros are localized very close to dashed lines.

Figure 4 documents numerical results for the curve of off-critical zeros (full squares) interconnecting the pair of right and left edge zeros, denoted as 2a and 2b in Figure 1. The evolution of the component ρ_x along the curve is indicated by numbers with short lines attached; by definition

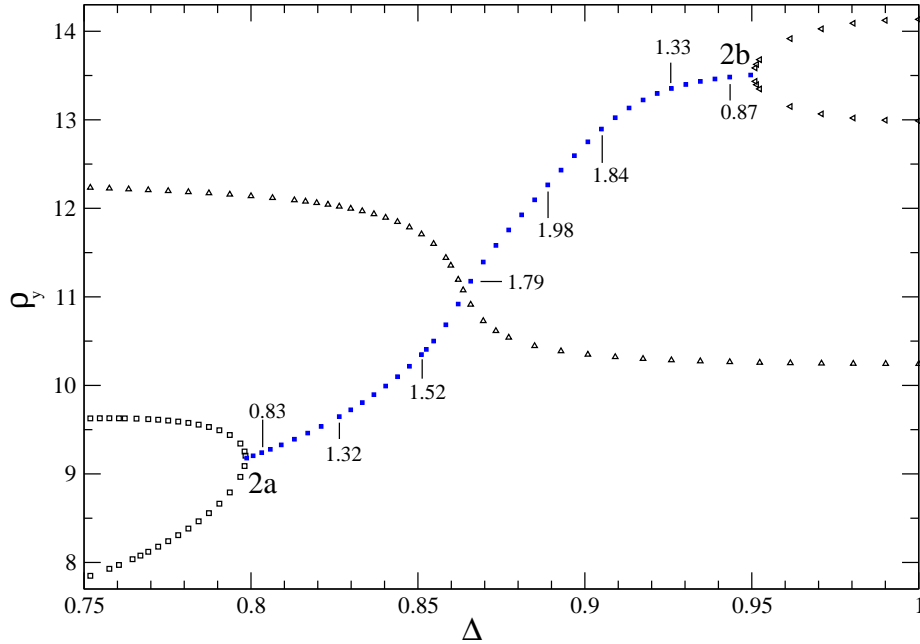


Figure 4. Numerical results for the curve off-critical zeros (full squares) between the right edge point 2a (lying on the curve of critical zeros represented by open squares) and the left edge point 2b (lying on the curve of critical zeros represented by open triangles). The evolution of the component ρ_x along the curve is indicated by short lines. At each point of the curve there exists another solution with the component $1 - \rho_x$.

of critical zeros, $\rho_x = \frac{1}{2}$ at the edge points 2a and 2b. Note that at each point of the curve there exists another solution with the component $1 - \rho_x$. The intersection of the curve of off-critical zeros (full squares) with $\rho_x \neq \frac{1}{2}$ and the curve of critical zeros (open triangles) with $\rho_x = \frac{1}{2}$ is artificial because the corresponding components ρ_x do not coincide.

Comparison of our asymptotic formulas and analytic data obtained directly. A check of the asymptotic formulas (4.3) and (4.4) for the curve of off-critical zeros close to a left edge zero was made for the edge point denoted as 3b in Figure 1, similarly as in the previous case of the expansion formula (3.17) for the curve of critical zeros. The expected dependences

$$\delta\rho_x(\Delta) = \pm 4.87411\sqrt{\Delta^* - \Delta}, \quad -\delta\rho_y(\Delta) = 22.493(\Delta^* - \Delta) \quad (4.5)$$

are reproduced very well by fitting numerical data, namely the prefactor obtained for $\delta\rho_x$ equals to 4.87412 and the prefactor for $-\delta\rho_y$ is estimated to 22.498. The agreement of the asymptotic relations (4.5) (dashed lines) with the numerical data (open symbols) is pictured in Figure 5.

4.2. Real off-critical zeros

In this section, we are interested in real off-critical zeros. It has already been mentioned that the critical zero numbered by 1 in Figure 1, lying on the Δ -axis, is a left edge zero because the curve of critical zeros passes across the Δ -axis into the lower quadrant in a reflection-symmetrical way.

Numerical observations. The imaginary part of this point $\rho_y^* = 0$ as well as its associated

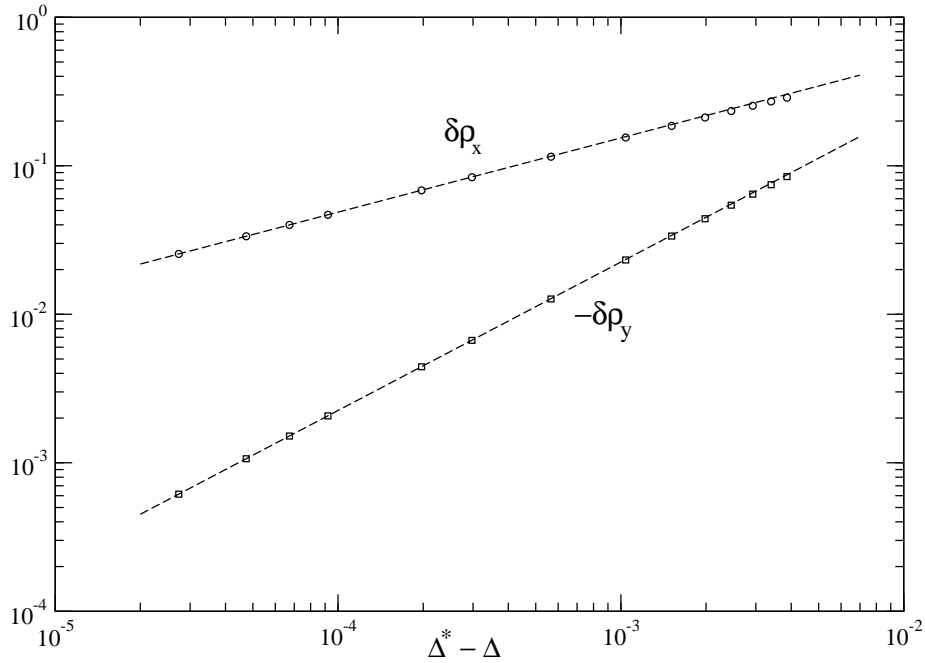


Figure 5. The log-log plot of numerical and analytic data for the curve of off-critical zeros going from the left edge denoted as 3b in Figure 1. Numerical dependences of $\delta\rho_x$ (open circles) and $-\delta\rho_y$ (open squares) on the small deviations from the edge point $\Delta^* - \Delta$ are compared with the analytic predictions (4.5) represented by dashed lines.

parameter Δ_c^* fulfill Eqs. (3.5) and (3.3) provided that

$$-2 + \int_0^1 \left[\theta_3(e^{-\pi t \Delta_c^*}) \theta_3(e^{-\pi t / \Delta_c^*}) - \frac{1}{t} \right] \frac{dt}{\sqrt{t}} = 0. \quad (4.6)$$

This equation obviously corresponds to $Z(1/2, \Delta_c^*) = 0$ (see (2.1) and (2.2)). Using the work of Montgomery [20] (recently recovered by Faulhuber and Steinerberger in [15]), we can show the following result.

Lemma 4.4. *Equation (4.6) admits a unique solution Δ_c^* on $(0, 1]$.*

Proof. It has been shown in [15, 20] that, for all $t > 0$, the function $\Delta \mapsto \theta_3(e^{-\pi t \Delta}) \theta_3(e^{-\pi t / \Delta})$ is strictly decreasing on $(0, 1)$. Furthermore, for $\Delta = 1$ we have

$$-2 + \int_0^1 \left[\theta_3(e^{-\pi t})^2 - \frac{1}{t} \right] \frac{dt}{\sqrt{t}} \approx -1.9501325 < 0.$$

To study the opposite $\Delta \rightarrow 0$ limit, we recall that $Z(s, \Delta)$ is related to the Epstein zeta function $\zeta^{(2)}(s, \Delta)$ via equation (2.1) and the small- Δ behavior of $\zeta^{(2)}(s, \Delta)$ is given by the asymptotic relation (3.29) where the $p = 2$ error term of the order $\mathcal{O}(\Delta)$ can be neglected in the limit $\Delta \rightarrow 0$. Thus one arrives at the asymptotic relation

$$Z(s, \Delta) \underset{\Delta \rightarrow 0}{\sim} \frac{1}{\Delta^s} \frac{1}{\pi^{\frac{1}{2}-s}} \Gamma\left(\frac{1}{2} - s\right) \zeta(1 - 2s) + \frac{1}{\Delta^{1-s}} \pi^{\frac{1}{2}-s} \Gamma\left(s - \frac{1}{2}\right) \zeta(2s - 1)$$

which exhibits the required duality symmetry (2.4). Consequently,

$$\lim_{s \rightarrow \frac{1}{2}} Z(s, \Delta) = \frac{\gamma - \log(4\pi\Delta)}{\sqrt{\Delta}},$$

where $\gamma = 0.5772156\dots$ is the Euler-Mascheroni constant. Thus,

$$Z\left(\frac{1}{2}, \Delta\right) \underset{\Delta \rightarrow 0}{\sim} -\frac{\log \Delta}{\sqrt{\Delta}} \rightarrow +\infty.$$

It follows that Δ_c^* is unique and the proof is complete. \square

As is seen in Table 1, the numerical solution of this equation is $\Delta_c^* \approx 0.141733239663887$. According to our numerical observations:

- (1) it turns out that the curve of off-critical zeros going out of the critical edge zero 1 stays on the Δ -axis, i.e. $\rho_y = 0$.
- (2) As concerns the coupled equations for off-critical zeros (2.8) and (2.9), the second one is automatically fulfilled for $\rho_y = 0$ while the first one implies

$$-\left(\frac{1}{1+2\delta\rho_x} + \frac{1}{1-2\delta\rho_x}\right) + \int_0^1 \cosh(\delta\rho_x \log t) \left[\theta_3(e^{-\pi t\Delta}) \theta_3(e^{-\pi t/\Delta}) - \frac{1}{t} \right] \frac{dt}{\sqrt{t}} = 0. \quad (4.7)$$

This equation has two conjugate *real* solutions for $\delta\rho_x$ and $-\delta\rho_x$ (or, equivalently, ρ_x and $1 - \rho_x$), only if $0 \leq \Delta < \Delta_c^*$ as observed in Figure 6.

- (3) The value of ρ_x is $\frac{1}{2}$ at the critical edge point 1 corresponding to $\Delta = \Delta_c^*$. As observed again in Figure 6, decreasing the value of $\Delta < \Delta_c^*$, the two values of ρ_x split and tend to the borders 0 (down branch) and 1 (up branch) of the critical strip in the limit $\Delta \rightarrow 0$.

Heuristic derivation of Δ_c^* from small Δ approximation. It is useful to test how Eq. (3.32), which is accurate but certainly only approximate for complex zeros (see Table 2), works in the present case of real off-critical zeros. Writing $\rho = \frac{1}{2} + \delta\rho_x$ in (3.32), one gets

$$\left(\frac{\Delta}{\pi}\right)^{2\delta\rho_x} = -\frac{\Gamma(-\delta\rho_x)\zeta(-2\delta\rho_x)}{\Gamma(\delta\rho_x)\zeta(2\delta\rho_x)}. \quad (4.8)$$

The expansion of both sides of this equation to the first order in small $\delta\rho_x$ must be consistent at $\Delta = \Delta_c^*$: as $\delta\rho_x \rightarrow 0$ we have

$$\left(\frac{\Delta^*}{\pi}\right)^{2\delta\rho_x} = 1 + 2 \log\left(\frac{\Delta_c^*}{\pi}\right) \delta\rho_x + \mathcal{O}(\delta\rho_x^2), \quad (4.9)$$

$$-\frac{\Gamma(-\delta\rho_x)\zeta(-2\delta\rho_x)}{\Gamma(\delta\rho_x)\zeta(2\delta\rho_x)} = 1 + 2[\gamma - 2\log(2\pi)]\delta\rho_x + \mathcal{O}(\delta\rho_x^2). \quad (4.10)$$

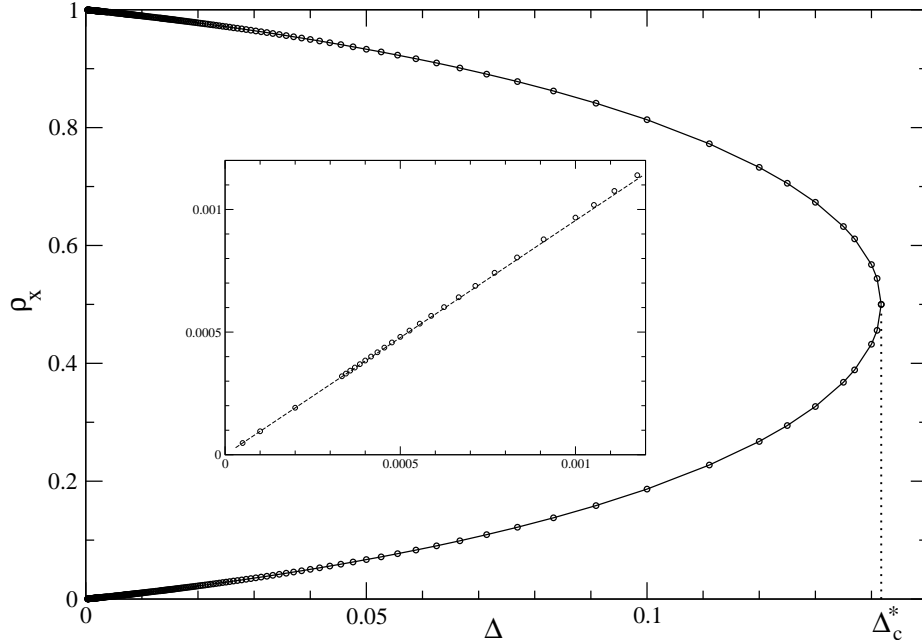


Figure 6. The dependence of the ρ_x -component of real off-critical zeros ($\rho_y = 0$) on the anisotropy parameter Δ , calculated numerically by using equation (4.7). As explained in the text, $\rho_x = \frac{1}{2}$ at $\Delta_c^* \approx 0.141733239663887$ and there are two conjugate solutions ρ_x and $1 - \rho_x$ for $0 < \Delta < \Delta_c^*$. As $\Delta \rightarrow 0$, the two values of ρ_x tend to the borders 0 (the down branch) and 1 (the up branch) of the critical strip. The inset concerns the down branch and the region of small Δ where numerical data for ρ_x versus Δ (open circles) satisfy the asymptotic relation $\rho_x \sim (3/\pi)\Delta$ (dashed line).

Consequently, it must hold that

$$\Delta_c^* = \frac{e^\gamma}{4\pi}. \quad (4.11)$$

We checked that Δ_c^* evaluated by using this analytic relation coincides with the previous numerical estimate $\Delta_c^* \approx 0.141733239663887$ obtained from the exact Eq. (4.6) by at least 22 decimal digits; to go further a computer facility more powerful than the one at our disposal is needed. This indicates that the result (4.11) might be exact which is difficult to prove directly by using (4.6). We have stated the corresponding open problem as Conjecture 1.1.

Approximation in the $\rho_x, \Delta \rightarrow 0$ regime and comparison with numerical data. As concerns the accuracy of the real off-critical zeros implied by Eq. (4.8), for various values of Δ from the interval $(0, \Delta_c^*)$ they coincide with the ones obtained from the exact Eq. (4.7) up to 27 decimal digits, which supports the hypothesis that the real off-critical zeros generated from Eq. (4.8) are exact.

For the down branch in Figure 6, to obtain the asymptotic tendency of ρ_x to 0 as $\Delta \rightarrow 0$ by using the relation (4.8), one writes $\delta\rho_x = \rho_x - \frac{1}{2}$ and expands the right-hand side in small ρ_x :

$$-\frac{\Gamma\left(\frac{1}{2} - \rho_x\right) \zeta(1 - 2\rho_x)}{\Gamma\left(\rho_x - \frac{1}{2}\right) \zeta(2\rho_x - 1)} = \frac{3}{\rho_x} + o(1), \quad \text{as } \rho_x \rightarrow 0. \quad (4.12)$$

Consequently, again as $\Delta \rightarrow 0$

$$\rho_x = \frac{3}{\pi}\Delta + o(1). \quad (4.13)$$

As is seen in the inset of Figure 6, numerical data (open circles) agree well with this analytic prediction (dashed line).

Remark 4.5. *With regard to the symmetry $\Delta \rightarrow 1/\Delta$ of basic equations for zeros of $\zeta^{(2)}(s, \Delta)$, there exists a pair of continuous curves of real off-critical zeros also for each $\Delta > 1/\Delta_c^* \approx 7.055507955448192$.*

Acknowledgment

Ladislav Šamaj and Igor Travěnek acknowledge the support received from VEGA Grant No. 2/0092/21.

References

- [1] T.M. Apostol, An elementary view of Euler’s summation formula, Amer. Math. Monthly 106 (1999) 409–418.
- [2] S. Baier, K. Srinivas, U.K. Sangale, A note on the gaps between zeros of Epstein’s zeta-functions on the critical line, Funct. Approx. Comment. Math. 57 (2017) 235–253.
- [3] P.T. Bateman, E. Grosswald, On Epstein’s zeta function, Acta Arithmetica 9 (1964) 365–373.
- [4] R.J. Baxter, Exactly solved models in statistical mechanics, Academic Press, London, 1982.
- [5] X. Blanc, M. Lewin, The crystallization conjecture: a review, EMS Surveys Math. Sci. 2 (2015) 255–306.
- [6] E. Bogomolny, P. Leboeuf, Statistical properties of the zeros of zeta functions - beyond the Riemann case, Nonlinearity 7 (1994) 1155–1167.
- [7] E. Bombieri, D.A. Hejhal, Sur des zeros des fonctions zêta d’Epstein, Comptes Rendus Acad. Sci. Paris 304 (1987) 213–217.
- [8] J.M. Borwein, M.L. Glasser, R.C. McPhedran, J.G. Wan, J.L. Zucker, Lattice Sums Then and Now, Table 1.6, pp. 60-62, Cambridge University Press, Cambridge, 2013.
- [9] J.S. Brauchart, Optimal discrete Riesz energy and discrepancy, Unif. Distrib. Theory 6 (2011) 207–220.
- [10] H. Davenport, H. Heilbronn, On the zeros of certain Dirichlet series I, J. London Math. Soc. 11 (1936) 181–185.
- [11] E. Elizalde, A. Romeo, Regularization of general multidimensional Epstein Zeta-functions, Rev. Math. Phys. 1 (1989) 113–128.
- [12] V. Ennola, On a problem about the Epstein zeta function, Proc. Camb. Philos. Soc. 60 (1964) 855–875.
- [13] P. Epstein, Zur Theorie allgemeiner Zetafunktionen, Math. Ann. 56 (1903) 615–644.
- [14] P. Epstein, Zur Theorie allgemeiner Zetafunktionen II, Math. Ann. 63 (1907) 205–216.
- [15] M. Faulhuber, S. Steinerberger, Optimal Gabor frame bounds for separable lattices and estimates for Jacobi theta functions, J. Math. Anal. Appl. 445 (2017) 407–422.

- [16] I.S. Gradshteyn, I.M. Ryzhik, Table of Integrals, Series, and Products, 6th edn., Academic Press, London, 2000.
- [17] M. Jutila, K. Srinivas, Gaps between the zeros of Epstein's zeta-functions on the critical line, *Bull. London Math. Soc.* 37 (2005) 45–53.
- [18] A. Lander, The Zeros of the Dirichlet beta function encode the odd primes and have real part $1/2$, *Preprints 2018*, 2018040305 (doi: 10.20944/preprints201804.0305.v1).
- [19] R.C. McPhedran, Zeros of lattice sums: 1. Zeros of the critical line, *arXiv:1601.01724* (2016).
- [20] H.L. Montgomery, Minimal Theta Functions, *Glasg. Math. J.* 30 (1988) 75–85.
- [21] H.S.A. Potter, E.C. Titchmarsh, The zeros of Epstein's zeta functions, *Proc. London Math. Soc.* 39 (1935) 372–384.
- [22] B. Riemann, Über die Anzahl der Primzahlen unter einer gegebenen Grösse, *Monats-berichte der Berliner Akademie* (1859) 671–680.
- [23] L. Šamaj, Z. Bajnok, *Introduction to the Statistical Physics of Integrable Many-body Systems*, Cambridge University Press, Cambridge, 2013.
- [24] H.M. Stark, On the zeros of Epstein's zeta function, *Mathematika* 14 (1967) 47–55.
- [25] I. Travěnek, L. Šamaj, Generation of off-critical zeros for hypercubic Epstein zeta functions, *Appl. Math. Comput.* 413 (2022) 126611.